U.P.B. Sci. Bull., Series D, Vol. 88, Iss. 3, 2026 ISSN 1454-2358

MODAL ANALYSIS AND STRUCTURAL STRENGTH EVALUATION OF KEY COMPONENTS IN ROLLING MILL MAIN DRIVE SYSTEM UNDER INSTABILITY CONDITIONS

Ran LI[1], Chongyi GAO[2,*], Aoyun WANG[3]

As an important device for transmitting motion and torque, the running stability and structural reliability of the rolling mill's main drive system have a crucial impact on productivity and products quality during the rolling process. The numerical simulation on instability mode of the main drive system of rolling mill and the structural strength of key parts is studied. Firstly, according to the principle of energy equivalence, a geometric model of the main drive system of the rolling mill is established. Then, using FEM simulation, the critical speeds of the main drive system are calculated, and the relationships between the critical speed and modal frequency are obtained. Next, the resonance modes caused by the critical speed are carried out, and to get the inherent vibration characteristics under the instability mode. Finally, the strength analysis of the weak links is carried out, to determine the failure causes of the damageable parts. The results provide a certain theoretical reference to control instability vibration and optimize key parts of the main drive system.

Key words: Main Drive System; Critical Speed; Modal Analysis; Strength Analysis; Distribution Gears

1. Introduction

With the rapid development of the metallurgy industry, it becomes important to place higher demands at the rolling mill speed. However, blind pursuit of speed will result in poor stable rolling production. In particular, the instability-induced vibrations phenomena caused by certain speeds not only severely affect the processing precision but also slow down the service life of parts in rolling mill systems [1-3], hence it is important to urgently tackle this problem of the speed-induced instability vibrations in rolling mills.

Rolling mill instability vibrations have attracted attention of the scientific community. Since vibration patterns are complex and inevitable, once the

[1] Lecturer, Key Laboratory of Digital Design and Process Simulation of Intelligent Equipment, Tangshan University, China, e-mail: liran@tsc.edu.cn

[2] Associate Prof, Key Laboratory of Digital Design and Process Simulation of Intelligent Equipment, Tangshan University, China; National Engineering Research Center for Cold Rolling Plate and Strip Equipment and Process Technology, Yanshan University, China, e-mail: chongyigao@tsc.edu.cn

[3] College of Mechanical and Electrical Engineering, Tangshan University, China, e-mail: 739016532@qq.com

instability vibration occurs, it will bring substantial financial losses to various users [4-9]. Li et al. proposed a torsional vibration model for the main drive system of cold continuous rolling mills. Multiscale and numerical methodologies were used to study the combined harmonic dynamics [10]. Zhao et al. introduced a nonlinear torsion flutter model for cold rolling mill drive systems with structural clearance and the rotation speed fluctuation and studied its nonlinear dynamic behavior under speed fluctuating excitation [11]. Liu et al. proposed a damper controller device to reduce the torsional vibration amplitudes in rolling mill drives [12]. Hou et al. proposed coupled vertical-torsional nonlinear vibration model in four-roll mills with vertical and torsional roller vibrations and studied their coupled dynamics [13]. Sun et al. applied combined control combining data analysis, vibration characteristic evaluation and suppression to deal with high-speed rolling vibrations and product quality changes in cold continuous rolls [14]. Ogama et al. believed that adjusting torsional vibration parameters such as moment of inertia can regulate the resonance and anti-resonance characteristics of the system and thus has the potential to reduce the transient torsional vibration of the system [15]. Amer et al. adopted an active control method to control the torsional vibration of nonlinear torsional vibration of rolling system [16]. Patel et al. developed an efficient 3D nonlinear chatter vibration model for cold rolling mills by coupling the mill structural dynamics, obtained via the simplified-mixed finite element method, with a rolling process (roll-bite mechanics) model [17].

Our research team has conducted preliminary studies on the vibration behavior of rolling mill main drive systems. Through numerical simulations, we investigated torsional vibration mechanisms in the main drive system, analyzed electromechanical coupling effects, and examined nonlinear vibrations in steel strips influenced by torsional dynamics. This provides fundamental theory for vibration analysis and control in actual rolling [18]. In this paper, vibration issues in rolling mill main drives, numerical simulations on account of instability modes and structural strength analysis of critical elements under wear are discussed.

2. Model establishment of the main drive system in the rolling mill

This study developed a geometric model for the F3 main drive system of a 1580PC continuous rolling mill at a steel plant, which has a maximum rolling force of 23,222 kN [19]. In other words, the F3 main drive system of a 1580PC continuous rolling mill refers to the main drive system of the 3rd stand.

The system features a motor-driven configuration: a coupling with safety bolts drives a distribution gear, which in turn rotates the upper and lower main shafts. These shafts ultimately drive the upper and lower rolls, as shown in Figure 1.

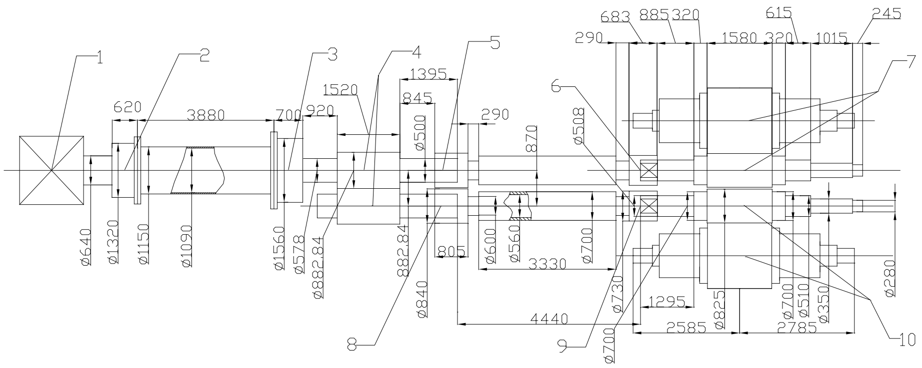

1. Motor rotor 2. Input end of coupling shaft 3. Output end of coupling shaft

4. Gear 5. Upper spindle input shaft 6. Upper spindle output shaft

7 Upper roll 8 Lower spindle input shaft 9 Lower spindle output shaft 10 Lower roll

Fig.1 Overall structure diagram of F3 main drive system

Based on the energy equivalence principle and system symmetry characteristics, the main drive system of a branch-type rolling mill is equivalently simplified into a series-parallel geometric model. After this equivalence transformation, the branch meshing parameters transmitted by the distribution gears become twice their original values. Specifically, the rotational inertia of corresponding components doubles, and the torsional stiffness of corresponding shaft segments also doubles. The detailed geometric model of this equivalent simplification is illustrated in Figure 2.

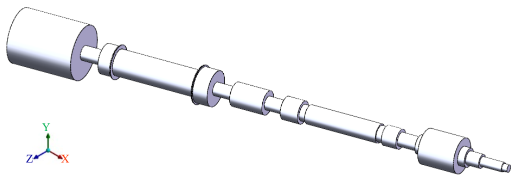

Fig.2 Geometric model of main drive system of rolling mill

3. Calculation and analysis of critical speed

According to rotor dynamics theory, a rotational speed is considered a critical speed when it matches the frequency of a specific rotor mode [20]. While the main drive system contains multiple mode frequencies corresponding to various critical speeds, determining which specific mode frequency constitutes the rotor's critical speed requires further analysis.

To determine the critical speed of the rolling mill's main drive system and analyze its vibration characteristics, the geometric model of the system shown in Figure 2 was imported into ANSYS software. The axial motion trajectory was extracted to reconstruct the model, and the Campbell diagram of the main drive system was subsequently generated, as illustrated in Figure 3.

Figure 3 presents the Campbell diagram of the main drive system for a rolling mill, where the horizontal axis represents system speed and the vertical axis indicates modal frequency, the red heavy solid line denotes the synchronous excitation line. This figure shows the relationship between system speed and modal frequency variations. When subjected to impact loads, the system generates orbital motion around the axis, known as vortex. The diagram shows FW (Forward Vortex Frequency Curve) and BW (Backward Vortex Frequency Curve). The impact load stimulates the free vibration, accompanied by the simultaneous occurrence of forward and backward vortex. According to rotor dynamics, this critical speed occurs when the rotor speed is like the modal frequency. Although the synchronous excitation curve intersects forward and backwards modal velocity curves, the imbalance does not produce backward vortex resonance if the direction of the vortex opposes rotor rotation. Therefore, the intersection points between forward vortex frequency curves and the synchronous excitation line are identified as the critical speeds of the rolling mill's main drive system.

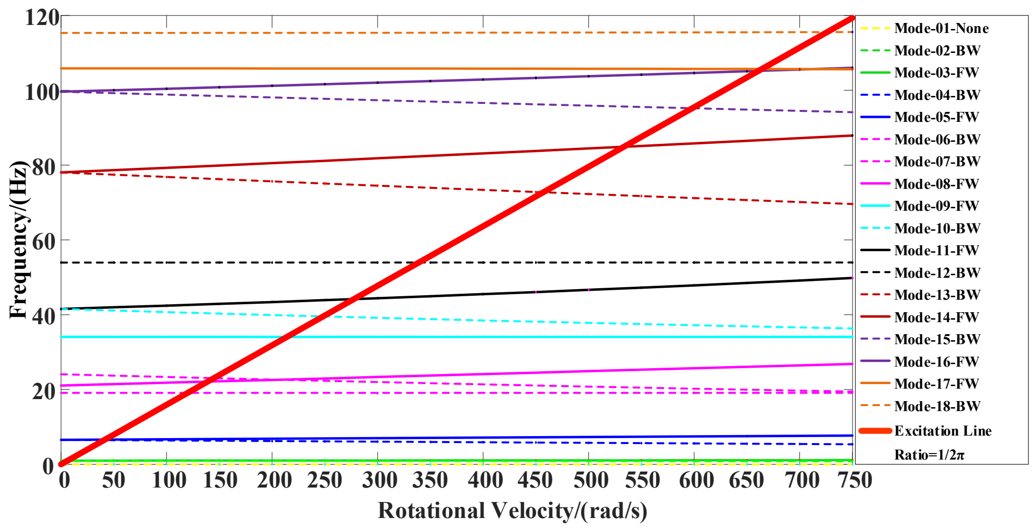

Fig.3 Campbell diagram of main drive system of rolling mill

In order to further analyze the specific correspondence between critical speed and modal frequency, the numerical forward vortex sampling is extracted for comparative analysis, as shown in Table 1.

Table 1

Correspondence between critical speed and modal frequency

name	Critical speed (rad/s)	modal frequency(Hz)			
Sampling speed		0	250	500	750
1	6.23	0.9902	1.0329	1.0761	1.1196
2	41.53	6.545	6.9356	7.7312	7.6687
3	138.89	21.069	23.069	24.905	26.824
4	214.09	34.074	34.074	34.074	34.074
5	277.60	41.546	41.546	46.646	49.814
6	533.51	78.048	78.048	84.456	87.914
7	660.94	99.633	99.633	103.75	106.01
8	664.08	105.86	105.86	105.76	105.65

As shown in Table 1, the modal frequencies of each order increase gradually, with their critical speeds coinciding with the modal frequency curves, indicating instability resonance occurs at these equal values. In actual rolling operations, the spindle rotation speed in the main drive system of the rolling mill should remain below 150 rad/s. Comparative analysis of sampled data reveals potential critical speeds of 6.23 rad/s, 41.53 rad/s, and 138.89 rad/s-precisely the dangerous speeds that could trigger resonance modes.

4. Modal analysis of the main drive system in the rolling mill

The critical speed of the system may cause great potential harm, and in serious cases, the key parts will break instantly. Therefore, it is particularly necessary to analyze the unstable mode of the main drive system of the rolling mill caused by the critical speed and obtain the inherent vibration characteristics under this mode.

In actual rolling processes, excitation frequencies are predominantly low, so only modal vibrations below 20 Hz are analyzed. The modal analysis incorporates motor drive characteristics by imposing constraints on X, Y, and Z-axis translations at the motor end, along with rotational restrictions in the Y and Z directions. The resulting modal vibration mode cloud diagrams are shown in Figure 4.

By using the ANSYS finite element software for simulation, exaggerated deformation contour maps can be obtained to display deformation trends. From the deformation trend analysis of the mode cloud diagram in Figure 4, Figure 4.a-4.c respectively show the bending vibration, bending-torsion vibration and torsional vibration modes of the main drive system of the rolling mill.

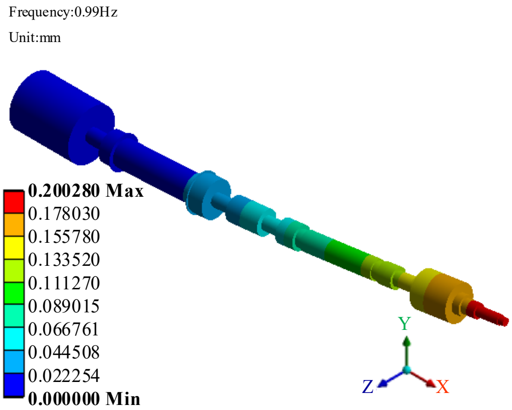

a. Bending vibration mode shape

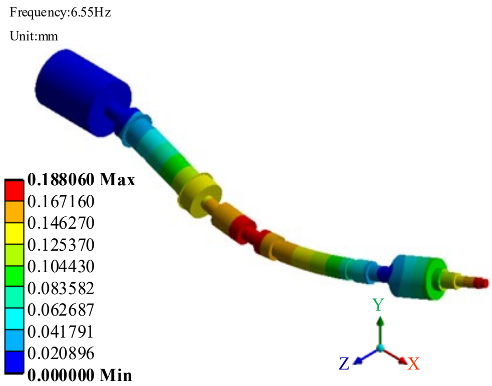

b. Bending-torsional vibration mode shape

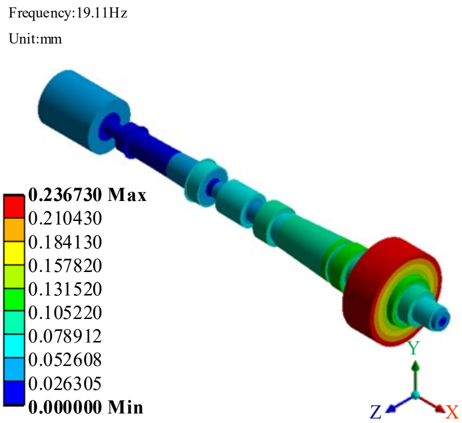

c. Twist vibration mode shape

Fig.4 Vibration mode contour of main drive System of rolling mill

As shown in Fig.4.a of the bending vibration mode shape cloud diagram, when the natural frequency reaches 0.99 Hz, the main drive system of the rolling mill exhibits bending vibrations along the Y-axis direction. Significant deformation occurs at the roll end, with the deformation gradually increasing in the positive X-axis direction. Although this low-frequency mode is often overlooked during rolling operations, the motor speed may momentarily cross this frequency band during initial startup, causing intense vibrations at the roll end. Repeated passage through this frequency band could lead to fatigue fracture of the roll-end structure, posing significant safety hazards to production.

Fig.4.b shows that at 6.55 Hz the main drive system has bending-torsion coupling vibrations and large deformation occurs at both the equivalent distribution gear and roll neck. The equivalent distribution gears shows the largest deformation as this component is crucial in transmitting and distributing the torque smoothly in the rolling mill transmission system. Resonance triggered by

excitation frequencies matching or coming close to the natural frequency would directly destabilize the torque transmission and cause severe economic losses.

Fig. 4.c shows that when the inherent frequency is 19.11 Hz, the main drive system has torsional vibrations along the X-axis rotation direction with the roll body undergoing large deformations with a maximum displacement of 0.24mm. This indicates that the roll is very sensitive to structural failure under this mode. The main drive of this model rolling mill has a distribution gear, which is prone to scuffing at very high speeds. To avoid scuffing the speed of the rotational period of production must be no more than 50 rad/s. While the torsion modes cause significant deformation and displacement of components, the resonance frequency of the modes during real rolling is much higher than the excitation frequency, so the torsion modes can be hard to induce.

It is seen that the first 3 modes of the main drive system have natural frequencies of 0.99 Hz, 6.55 Hz, and 19.11 Hz that coincide with critical speeds indicated by the modal frequency curve.The bending mode and the torsional bending mode are both within the rolling speed region. In real production, excitation frequencies should not be matched or approached natural frequencies, and greater structural strength of parts prone to deformation, such as distribution gears and rolls, can help in reducing safety threats.

5. Strength analysis of key components

Based on the previous modal analysis results, a strength analysis is further conducted on components with maximum deformation in the main drive system. By applying critical rotational speeds to the key weak links, the areas under maximum stress and the causes of damage are identified.

5.1 Rollers and Flat Head Sleeves

Rollers are the primary working components and tools in rolling mills that enable continuous plastic deformation of metals, consisting mainly of a roll body, roll neck, and shaft end. In the transmission system, torque is primarily transmitted through the connection between the flat end of the roll and the flat headgear, indicating that this connection structure bears significant loads. This section uses ANSYS finite element software to conduct structural force analysis. It applies rolling torque $T = 1.095 \times 10^9 \mathrm{N \cdot mm}$ to the model to examine force variations under maximum rolling force conditions. The components are made of S45C, which has a yield strength of 550 MPa and a bending fatigue limit of 388.3 MPa, as shown in Figure 5.

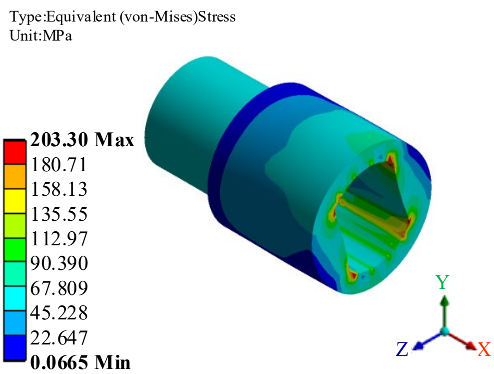

a. Flat headgear

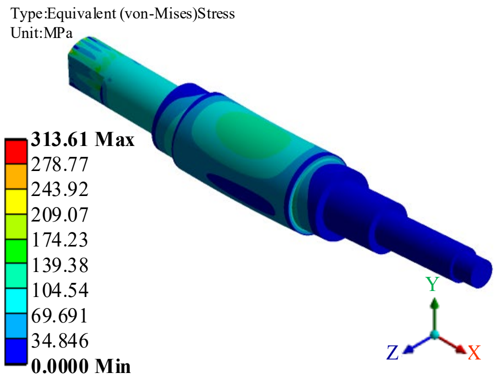

b. Roll

Fig.5 The equivalent stress contour of flat headgear and roller

Figure 5 displays the equivalent stress cloud diagrams of the flat headgear and roller. The analysis reveals that the flat headgear experiences maximum stress of 203.3MPa, primarily concentrated at the junction between its internal plane and curved surface. The roller demonstrates maximum stress of 313.6MPa, predominantly localized at its flat end-corresponding to the contact position of the flat headgear's region of maximum stress. This indicates significant stress concentration at the matching edge transition between the flat headgear and roller's flat end, aligning with actual wear patterns. According to manufacturer specifications, both components' yield strength $\sigma_s = 550\text{MPa}$, allowable stress limits $[\sigma] = 322.7\text{MPa}$, and maximum equivalent stresses remain below permissible thresholds, confirming compliance with strength requirements under rated torque. However, the roller's flat end stress approaching the allowable limit suggests inadequate safety margins. Under unexpected conditions like sudden vibrations, this critical gap may compromise fatigue strength performance.

5.2 Distribution Gear

The distribution gear is located at position 4 as shown in Figure 1. The distribution gear of F3 main drive system adopts 1:1 herringbone gear drive, with module of 28 mm, tooth number of 25, pressure angle of 20°, center distance of 800 mm, face width of 500 mm and pitch diameter of 700 mm. The gear material is 17CrNiMo6.

The distribution gear is a key component in the main drive system of the rolling mill to distribute torque and realize smooth rolling. Compared with the working conditions of flat head sleeve and working roll, the distribution gear is more complex and has a certain time correlation. Therefore, the transient dynamics theory is used to analyze the strength of the distribution gear.

Based on actual test data, A rotational speed boundary condition of 10°/s is applied to the input end and then the maximum rolling torque $T=\pm 1.095\times 10^{9}\,\mathrm{N\cdot mm}$ in opposite directions is imposed on both gears, thus the time-domain stress curve for the distribution gear rotating 1/5 of a full circle is obtained, as shown in Figure 6. The analysis reveals that during the initial engagement phase, the equivalent stress experiences a sudden surge. After reaching t=0.21s, the equivalent stress shows a downward trend before rebounding to exhibit stable fluctuations.

As time progresses, when t=1.64s reaches its peak, the gear pair achieves complete meshing of the first pair of tooth profiles. Subsequently, the stress pattern exhibits periodic variations with identical cyclical characteristics. During the engagement the maximum stress is constant in the 339.79 – 514.16MPa range while still below the yield $\sigma_s = 980\mathrm{MPa}$, so the two gear pairs hold sufficient safety margins for the equivalent stresses to ensure compliance with the strength requirements at the rated torque.

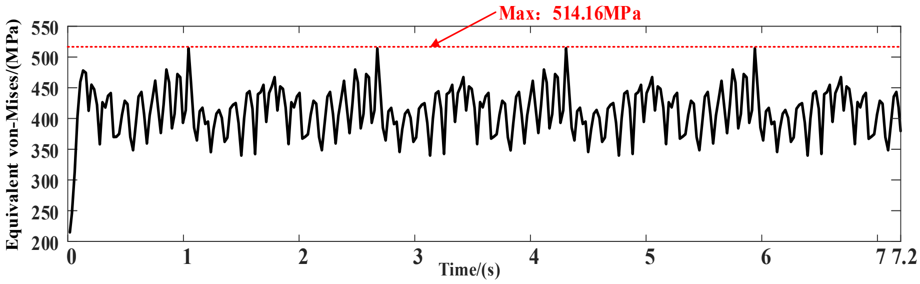

Fig.6 time domain response curve of stress of distribution gears

Since the distribution gear pair is helical and has a specific helix angle, when it shift torque in different spatial directions, it does not rely on one pair of tooth profiles coming into the meshing region along the tooth width. In order to further investigate the stress distribution during the gear pair meshing process, the stress cloud diagrams for t=4.92s and t=6.29s are used to analyze, as shown in Fig. 7-8.

Figures 7 and 8 show that the stress distribution at each moment mainly involves four pairs of gear tooth profiles in the meshing. The left and right meshing gears show periodic symmetric stress behavior, with maximum stress concentrated at the tooth tip and slowly falling toward the root. This demonstrates that gear stress is predominantly governed by contact strength, while tooth root bending strength remains relatively minor. Furthermore, smooth transmission during helical gear meshing requires fewer minimum teeth to avoid root cutting. Consequently, even at the tooth tip where stress peaks, the gears maintain strong stress reserve capacity.

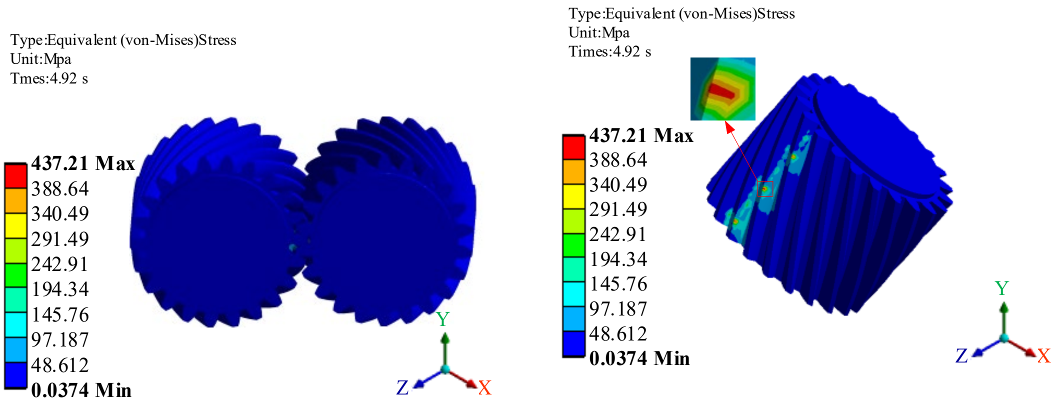

a. Gear pair meshing state equivalent stress cloud map b. Single gear meshing equivalent stress cloud map

Fig.7 When t=4.92 s, the equivalent stress contour under meshing condition

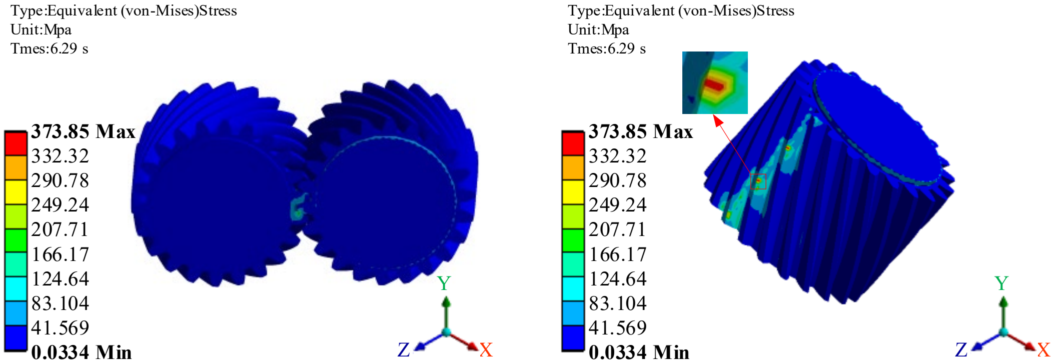

a. Gear pair meshing state equivalent stress cloud map b. Single gear meshing equivalent stress cloud map

Fig.8 When t=6.29 s, the equivalent stress contour under meshing condition

6. Conclusions

This study employs ANSYS finite element software to conduct theoretical analysis of instability modes in the main drive system of a rolling mill, while investigating the structural strength of vulnerable components. Numerical simulations reveal instability critical speeds of 6.23 rad/s, 41.53 rad/s, and 138.89 rad/s for the main drive system, all of which represent critical thresholds that can induce system resonance. Then the modal vibration characteristics corresponding to the speeds are studied, which illustrates that the resonance modes caused by 6. 23 rad/s, 41. 53 rad/s, 138.88 rad/s are bending vibration, bending-torsional vibration and torsional vibration respectively. Furthermore, a deformation maximum points of key components provide equivalent stress contour maps of flat-end bushing, roll and distribution gears. The analysis shows that these components display sufficient stress safety margins, some lack enough stress reserve capacity, which raises the question of possibly failure modes such as scuffing damage or fatigue failure due to high temperature, high pressure, and high speed. Specialized material strengthening treatment for critical components can reduce accident risks. The results provide useful theoretical references for vibration control and structural optimization of rolling mill drive system.

Acknowledgement

This study was supported by the High-level Talent Support Program of Hebei Province of China (No.C2024041).

REFERENCES

[1] *S. Chen, Y. Liu, Y. Wang, et al.* "Multi-dimension and multi-modal rolling mill vibration prediction model based on multi-level network fusion". Journal of Central South University, **vol. 31**, no.9, Sept. 2024, pp.3329−3348.

[2] *A. V. Kozhevnikov, A.`mirnov and I. A. Kozhevnikova, et al.* "Investigation of self-oscillations and the development of a procedure of stabilization of the process in a continuous mill for strip cold rolling". Metallurgist, **vol. 64**, no.12, Nov. 2020, pp.770–779.

[3] *O. Kurpe, V. Kukhar,* "Development and substantiation of proposals for modernization of plate rolling mill", Advance Manufacturing Processes VI, Interpartner -2024, Sept. 2024, pp. 535-544

[4] *Y. Kim, H. Park, and S. S. Lee, et al.* "Development of a mathematical model for the prediction of vibration in a cold rolling mill including the driving System". ISIJ International, **vol. 52**, no.6, 2012, pp.1135–1144.

[5] *S. Kapil, P. Eberhard, S. K. Dwivedy.* "Nonlinear dynamic analysis of a parametrically excited cold rolling mill". Journal of Manufacturing Science and Engineering, **vol.** 136, no.4, Aug 2014, pp. 041012

[6] *R. L. Shatalov, E. A. Maksimov.* "Analysis of asymmetric rolling efficiency for improving rolled strip accuracy". Metallurgist, **vol. 60**, no. 7-8, Nov. 2016, pp. 730-735.

[7] T. Matyja, B. Lazarz. "Selection of torsional vibration damper based on the results of simulation". Journal of Vibroengineering, vol. 17, no.8848, Mar. 2017, pp. 4069-4077.

[8] *V. A. Pimenov*. "Study of causes of vibrations in a continuous cold rolling mill". *Chernye Metally*, no. 3, 2022, pp.49–55.

[9] *D. He, T. Wang, Y. Liu, et al.* "Review of Theoretical Studies on Vibration in Strip Rolling Mill". Journal of Mechanical Engineering, vol. 60, no.7, Apr. 2024, pp.93-113.

[10] *L. Li, Y. Fan, C. Zhong*. "Combined harmonics dynamics characteristics for main drive system of cold rolling mill". Forging and Stamping Technology, **vol. 48**, no.11, Nov. 2023, pp 133-140.

[11] *W. Zhao, Z. Liu, D. Huang*. "Effect of rotating speed fluctuation on the stability of torsional chatter in cold rolling". Journal of Vibration and Shock, **vol. 40**, no.18, Sept. 2021, pp 228-236.

[12] *B. Liu, Y. Wang, J. Jiang, et al.* "Parameter design and characteristic analysis of torsional vibration damper for main drive system of rolling mill". Acta Metrologica Sinica, **vol. 41**, no.11, Nov. 2020, pp1391-1397.

[13] *D. Hou, D. Guo, X. Chen.* "A study on vertical-torsional coupled nonlinear vibration characteristics of 4-h rolling mill based on dynamic rolling force". Journal of Vibration and Shock, **vol. 39**, no.20, Oct. 2020, pp.106-112.

[14] *J. Sun, S. Chen, W. Yun, et al.* "Intelligent optimization control technology for key quality indexes and rolling stability of tandem cold rolling". Journal of Iron and Steel Research, **vol. 34**, no.12, Dec. 2022, pp.1387-1397.

[15] *A. Ogama, K. Adachi,* "Effect of inerter on frequency characteristic of multi-DOF torsional vibration system". Transactions of JSME, **vol. 83**, no. 848, Mar. 2017, pp. 441-446.

[16] *Y. A. Amer, A. T. El-Sayed, F. T. El-Bahrawy.* "Torsional vibration reduction for rolling mill's main drive system via negative velocity feedback under parametric excitation". Journal of Mechanical Science and Technology, **vol. 29**, no. 4, May 2015, pp. 1581-1589.

[17] *A. Patel, A. Malik, R. Mathews.* "Computational method to predict three-dimensional chatter vibration in cold rolling of flat metals." Journal of Manufacturing Science and Engineering, **vol. 145**, no4, Apr 2023, pp. 041004.

[18] *C. Gao, Y. Wei, H. Qin, et al.* "Research on mechanism and influential factors of torsional vibration of main drive electromechanical coupled system of rolling mill". Journal of Mechanical Strength, **vol.42**, no.4, Aug.2020, pp.966-970.

[19] *C. Gao.* Torsional vibration research of main driving system of rolling mill with impact of clearances and strip vibration, PhD Thesis, Yanshan University, 2015.

[20] *B. Wen, J. Gu, S. Xia, et al.* "Advanced rotor dynamics—theory, technology and applications", Mechanical Industry Press, 2000.